

Low-Frequency Electronic Noise in Exfoliated Quasi-1D TaSe₃ van Der Waals Nanowires

Guanxiong Liu¹, Sergey Rumyantsev^{2,3}, Matthew A. Bloodgood⁴, Tina T. Salguero⁴, Michael Shur² and Alexander A. Balandin¹

¹Nano-Device Laboratory (NDL) and Phonon Optimized Engineered Materials (POEM) Center, Department of Electrical and Computer Engineering, University of California – Riverside, Riverside, California 92521 USA

²Department of Electrical, Computer, and Systems Engineering, Center for Integrated Electronics, Rensselaer Polytechnic Institute, Troy, New York 12180 USA

³Ioffe Physical-Technical Institute, St. Petersburg 194021 Russia

⁴Department of Chemistry, University of Georgia, Athens, Georgia 30602 USA

Abstract

We report results of investigation of the low-frequency electronic excess noise in quasi-1D nanowires of TaSe₃ capped with quasi-2D *h*-BN layers. Semi-metallic TaSe₃ is a quasi-1D van der Waals material with exceptionally high breakdown current density. It was found that TaSe₃ nanowires have lower levels of the normalized noise spectral density, S_I/I^2 , compared to carbon nanotubes and graphene (I is the current). The temperature-dependent measurements revealed that the low-frequency electronic $1/f$ noise becomes the $1/f^2$ -type as temperature increases to ~400 K, suggesting the onset of electromigration (f is the frequency). Using the Dutta–Horn random fluctuation model of the electronic noise in metals we determined that the noise activation energy for quasi-1D TaSe₃ nanowires is approximately $E_P \approx 1.0$ eV. In the framework of the empirical noise model for metallic interconnects, the extracted activation energy, related to electromigration, is $E_A = 0.88$ eV, consistent with that for Cu and Al interconnects. Our results shed light on the physical mechanism of low-frequency $1/f$ noise in quasi-1D van der Waals semi-metals and suggest that such material systems have potential for ultimately downscaled local interconnect applications.

Keywords: quasi-1D materials; van der Waals materials; low-frequency noise; interconnects

The investigations of the two-dimensional layers and heterostructures revealed new physics and demonstrated promising applications [1-14]. Starting with graphene [3-5], and spreading to a wide range of layered van der Waals materials [6-10], successful isolation of individual atomic layers from their respective bulk crystals by mechanical exfoliation led to the fast growing research activities in the 2D materials. In contrast to the layered van der Waals materials that yield 2D crystals, materials, such as TaSe₃ and TiS₃ [15-17] yield the quasi-one-dimensional (1D) van der Waals crystal structures. These materials belong to the group of the transition metal trichalcogenides MX₃ (where M = Mo, W, and other transition metals; X = S, Se, Te). In the monoclinic crystal structure of TaSe₃, the trigonal prismatic TaSe₃ units form continuous chains extending along the *b* axis and leading to fiber- and needle-like crystals with anisotropic semi-metallic or metallic properties. The quasi-1D atomic threads are weakly bound in bundles by the van der Waals forces. As a consequence, the mechanical exfoliation of the MX₃ crystals results not in the 2D layers but rather in the quasi-1D van der Waals nanowires. We have recently demonstrated quasi-1D TaSe₃ nanowires with the record high current density exceeding $J_B \sim 10 \text{ MA/cm}^2$, which is an order of magnitude larger than that for the Cu interconnects [18].

In this Letter, we report on the excess low-frequency electronic noise in quasi-1D nanowires of TaSe₃ capped with the quasi-2D *h*-BN layers. The *h*-BN capping was used as a surface passivation protecting from environmental exposure. The measurements were performed in the temperature range from 300 K to 430 K in order to elucidate the physical mechanism of the low-frequency noise and determine the noise activation energies. The low-frequency noise is a ubiquitous phenomenon present in all kinds of electronic devices including field-effect transistors, diodes and interconnects [19-21]. The frequency dependence and temperature characteristics of the spectral density of the low-frequency noise have been used as reliability metrics for interconnects in Si complementary metal-oxide-semiconductor (CMOS) technology. The low-frequency noise data at elevated temperatures are directly correlated with the electromigration failure mechanisms in interconnects [22-24]. It was suggested that the low-frequency noise at high temperatures originates from the vacancy migration along the grain boundaries [22, 25]. Hence, the noise can reveal information on the electromigration failure of interconnects and metal thin films. The noise activation energies extracted from the two commonly accepted physical models, the Dutta–Horn model [21, 24] and the empirical noise model in metals [22, 26, 27], have shown an excellent agreement with the activation

energies obtained from the industry standard electromigration mean-time-to-failure (MTF) tests. These considerations explain additional practical motivations for investigation of the low-frequency noise in quasi-1D nanowires of TaSe₃, which exhibit promise as ultimately downscaled local interconnects owing to their single-crystal atomic thread structure and exceptionally high breakdown current density [18].

The bulk TaSe₃ crystals were synthesized by the chemical vapor transport (CVT) method and then were solvent exfoliated (see Methods). The high quality of both bulk and exfoliated quasi-1D TaSe₃ samples has been confirmed using a variety of experimental techniques including high-resolution transmission electron microscopy, Raman spectroscopy, energy dispersive spectroscopy, powder X-ray diffraction, and electron probe micro analysis, as reported previously [18]. The devices for the low-frequency noise measurement were fabricated by the mechanical exfoliation of the quasi-1D TaSe₃ nanowires on Si/SiO₂ substrates. We used the dry transferred *h*-BN flakes to protect the quasi-1D TaSe₃ nanowire channels from oxidation and chemical exposure during the fabrication processes. The devices were fabricated by standard e-beam lithography and e-beam metal evaporation [28]. In order to make an electrical connection to the quasi-1D channels we opened the contact area by dry etching the *h*-BN thin film and the underlying TaSe₃ nanowire while leaving the edge of quasi-1D channels in contact with the metal. Figure 1 (a) shows a high-resolution transmission electron microscopy (TEM) image of TaSe₃ crystal prepared by CVT method together with a schematic of the atomic plane arrangements. A scanning electron microscopy (SEM) of the long TaSe₃ nanowires is presented in Figure 1 (b). Figure 1 (c) is a SEM image of representative devices used for the current voltage (I-V) and electronic noise measurements.

[Figure 1 (a-c)]

Figure 2 presents typical I-V characteristics of the devices with different channel lengths. The perfectly linear I-Vs at low electric fields indicate a high-quality electrical contact between the metal electrode and the quasi-1D TaSe₃ nanowire. The *h*-BN capping was essential for achieving a good Ohmic contact between the metal electrodes and the TaSe₃ channel. The inset to Figure 2 shows an optical image of a representative device used in this study. The

light blue stripe between metal electrodes is the quasi-1D TaSe₃ nanowire while the green region is the *h*-BN capping layer. The red background is the Si/SiO₂ substrate.

[Figure 2]

The low-frequency noise measurements were performed both at UCR and RPI using in-house built experimental setups. The equipment included a “quiet” battery, a potentiometer biasing circuit, a low noise amplifier and a spectrum analyzer. The details of our noise measurement procedures have been reported elsewhere [28 - 29]. Figure 3 (a) shows a typical normalized noise spectral density $S_I/I^2 \propto 1/f^\gamma$ with $\gamma=1.16$ (here I is the channel source – drain current) in the TaSe₃ nanowires with the 20 nm × 110 nm cross-section. The measurements were performed at room temperature (RT). The noise spectral density was determined for the currents in the 1 μA – 5 μA range, which is sufficiently small to exclude the current induced effects such as electromigration. The latter is confirmed by the perfectly quadratic dependence of the noise spectral density on the source – drain current, i.e. $S_I \propto I^2$. The noise spectral density as a function of the source-drain current is shown in the inset to Figure 3 (a). The noise spectrum was collected for the two-terminal device. Since the contact resistance is very small compare to that of the channel, the contact noise was negligible.

The first interesting observation from the experimental data is that the noise level in TaSe₃ nanowires is rather low in comparison with other low-dimensional materials, such as carbon nanotubes and graphene, which also have been proposed as the interconnect applications. The normalized noise spectral density, S_I/I^2 , for TaSe₃ nanowires as a function of the resistance is shown in Figure 3 (b). The data points for carbon nanotubes [30-32] and graphene [29, 33] are presented for comparison. The guide line is the noise amplitude, $A=S_I/I^2 \times f$, which was empirically obtained for the carbon nanotubes [30]. The devices with a lower resistance tend to have a lower level of the low-frequency noise. As one can see, the noise level, expressed as S_I/I^2 , in quasi-1D TaSe₃ nanowires is about one order of magnitude lower than that in graphene [29, 33]. It is comparable to the lowest reported values for the carbon nanotubes [30-32]. Most of the tested carbon nanotube devices had a larger resistance and, as a result, a larger noise spectral density. The higher levels of $1/f$ noise typically are associated with a higher density of structural defects, as well as mechanical and electromigration damage [22, 25].

[Figure 3 (a-b)]

The resistivity of quasi-1D TaSe₃ nanowires increases with temperature, similar to other metallic materials. The inset to Figure 4 shows the resistivity change in the temperature range from 298 K to 450 K. The gradual and relatively slow resistance increase below 420 K is due to increasing electron–phonon scattering, which is common in metals. The sharp increase in resistance at the temperatures above 420 K is likely related to the onset of electromigration as commonly observed in the conventional interconnect reliability tests [24, 34]. The TaSe₃ nanowire noise spectral density and the frequency exponent γ rapidly grows with temperature (see Figure 4). The noise level at 378 K increases by a factor of $\times 10$ at 100 Hz and a factor of $\times 300$ at 1 Hz compared to that at 298 K. The noise magnitude grows faster at the lower frequencies, changing the type of the frequency dependence of the normalized noise spectral density, S_I/I^2 , at high temperature.

[Figure 4]

To better understand the evolution of the low-frequency noise with temperature, we plotted the frequency exponent γ and the normalized noise spectral density, S_I/I^2 , as the functions of temperature in the range from 298 K to 431 K. The experimental data points in Figure 5 (a-b) are shown for two representative devices with different channel cross-section areas at the frequency $f=10$ Hz. The frequency exponent γ increases from ~ 1.16 - 1.24 at 298 K to 1.72 - 1.75 at 350 K. At temperatures above 350 K, γ remains nearly constant at 1.71 - 1.75 (see Figure 5 (a)). In Figure 5 (b), one can see that the noise level increases by two orders of magnitude as temperature changes from 298 K to 400 K. The data in Figure 5 (b) suggest that the noise spectral density attains its maximum value at $T=400$ K and then reveal a saturation and a slowly decreasing trend. This behavior is analogous to that in thin films of Ag and Cu [35, 36]. In the region of the fast growth, $S_I/I^2 \sim T^s$ with $s=21$ for the shown data set for two representative devices (see Figure 5 (b)).

[Figure 5]

We now turn to the analysis of the experimental data using two different physical models. The Dutta–Horn model describes the temperature dependent low-frequency noise by the thermally activated random fluctuations [35]. Within this model, the noise spectral density, $S(f, T)$, can be approximated as

$$S(f, T) \propto \frac{kT}{2\pi f} D(E), \quad (1)$$

where $D(E)$ is the distribution density function of the activation energies E and $S(f, T)$ is the spectral noise density. In the limit of the constant $D(E)$ the model leads to the exact $1/f$ noise ($\gamma=1$). The experimentally observed deviations from $\gamma=1$ and temperature dependence of the noise indicate that $D(E)$ is not a constant. One should note here that the maximum in the $S(f, T)$ dependence on temperature does not always coincide with the maximum of $D(E)$ function. The temperature dependence of the frequency exponent γ is expressed as [35]

$$\gamma(T) = 1 - \frac{1}{\ln(2\pi f \tau_0)} \left(\frac{\partial \ln S(f, T)}{\partial \ln T} - 1 \right). \quad (2)$$

Here τ_0 is characteristic time constant referred to as the attempt escape time. In the original Dutta–Horn model, the time constant τ_0 was assumed to be $\sim 10^{-14}$ s which is the typical attempt escape time for random processes in solids. The exact value of τ_0 does not strongly affect the low-frequency noise analysis. The blue curve in Figure 5 (a) is a polynomial fit to the experimental data used in the further analysis.

In Figure 5 (b), the blue line is calculated using Eq. (2) with the approximated dependence of the frequency exponent γ on temperature shown in Figure 5 (a). One can see that the Dutta–Horn model describes accurately the temperature dependence of the noise for $T < 380$ K. The saturation or even the decrease of noise at higher temperatures cannot be explained by this model. The latter is likely related to the onset of another low-frequency noise mechanism. For this reason, applying of the Dutta–Horn model for temperatures above ~ 400 K has to be done with caution. The activation energy E_P , at which the distribution function $D(E)$ attains its peak is related to temperature as

$$E_p = -kT \ln(2\pi f\tau_0). \quad (3)$$

The activation energy distribution calculated from the noise data in metals usually has a peak at $E_p \approx 1$ eV [35]. Using the data for a representative device heated all the way to 430 K we determined that the energy distribution reaches its maximum at $E_p \approx 1.0$ eV for TaSe₃ nanowires as well (data set for “Device 1” in Figure 5 (b)). In a more conservative approach, increasing the temperature only to ~ 390 K, within the application domain of the Dutta–Horn model (data set for “Device 2” in Figure 5 (b)), we determine the low bound of the position of the maximum of the activation energy distribution function $D(E)$. This value is somewhat smaller but still close to ~ 1 eV.

The noise spectral density $S_I/I^2 \sim 1/f^\gamma$ with $\gamma \approx 2$ in metals is often attributed to the effects of electromigration. Although the detailed mechanism of the resistance fluctuations in metal films has not been established yet, many experiment indicate that the low-frequency noise, electromigration, and degradation in metals are related. The $1/f^\gamma$ noise spectral density with $\gamma \geq 2$, which appears at high temperatures, has been widely used to extract the electromigration activation energy for interconnects. The frequency exponents as high as $\gamma > 4$ have been reported [38]. Attributed to the vacancy migration, $1/f^\gamma$ noise has been proposed as a useful diagnostic tool [25]. It was found that the low-frequency noise at high temperature follows the empirical equation [22]

$$S(f) = \frac{Aj^3}{Tf^\gamma} \exp\left(-\frac{E_A}{kT}\right), \quad (4)$$

where A is a constant, j is the biasing current density and E_A is the activation energy related to electromigration. By measuring the temperature dependence of the noise spectrum one can extract the activation energy, E_A , from the Arrhenius plot of $T \times S(f)$. A large number of experiments have demonstrated that the E_A values extracted from the low-frequency noise measurements are very close to those obtained from the conventional mean-time-to-failure test for interconnects fabricated with different technology and various metals, including Al, Al alloys and Cu [21, 23, 24, 37]. The noise measurements have specific advantages over the conventional reliability tests, which require time-dependent resistance measurements of interconnects under high temperature and high current stress for long periods of time (typically from 10 to 100 hours for each set). The noise measurements can be conducted in much shorter

period of time. They are also be non-destructive. It was found that the noise level often increases rapidly before the sharp resistance increase, which was defined as the interconnect failure [24].

Figure 6 shows the Arrhenius plot of $T \times S_f / I^2$ vs. $1000/T$ for $f=10$ Hz. The extracted E_A of 0.88 eV is within the range reported for other metal films. Table I summarizes the electromigration activation energy estimated using the $1/f$ noise measurements for different interconnects. The values of the electromigration activation energy for the Cu and Al interconnects determined from the $1/f$ noise measurements are 0.76-1.10 eV and 0.67- 1.14 eV, respectively [21, 22, 24, 38, 39]. Our data suggest that quasi-1D TaSe₃ nanowires have similar E_A values. Considering the 10× fold higher current carrying capacity and a possibility of ultimate downscaling of the quasi-1D TaSe₃ van der Waals material, one can consider TaSe₃ to be a promising material for the nanoscale interconnects.

[Figure 6]

In conclusion, we investigated the low-frequency excess noise in quasi-1D nanowires of TaSe₃ capped with quasi-2D *h*-BN layers. The TaSe₃ nanowires have relatively low level of the $1/f$ noise in comparison with carbon nanotubes and other low-dimensional materials. The temperature dependent measurements revealed that the electronic excess noise becomes the $1/f^\gamma$ - type with $\gamma > 1$ as temperature increases. Using the Dutta–Horn random fluctuation model of $1/f$ noise in metals and empirical model for metallic interconnects we extracted the noise activation energy for quasi-1D TaSe₃ nanowires. Our results indicate that quasi-1D van der Waals materials have potential for the ultimately downscaled local interconnect applications.

METHODS

Material Preparation: TaSe₃ was prepared from elemental tantalum (12.0 mmol, STREM 99.98% purity) and selenium (35.9 mmol, STREM 99.99% purity) with iodine (~6.45 mg/cm³, J.T. Baker, 99.9% purity) as the transport agent. The tantalum/selenium mixture was ground and placed in a 17.78 x 1 cm fused quartz ampule (cleaned in concentrated nitric acid followed by annealing for 12 h at 900 °C). The charged reaction ampule was evacuated and

backfilled with Ar 3x while submerged in an acetonitrile/dry ice bath. The flame-sealed, ampule was placed in a three-zone, horizontal tube furnace heated at $20\text{ }^{\circ}\text{C min}^{-1}$ to the final temperature gradient of $700\text{ }^{\circ}\text{C}$ (hot zone) – $680\text{ }^{\circ}\text{C}$ (cool zone). The ampule was held at these temperatures for two weeks before cooling to room temperature. TaSe_3 crystals were removed carefully from the quartz ampule, and residual I_2 was removed by vacuum sublimation at $50\text{ }^{\circ}\text{C}$. The isolated yield of silver-black crystals was 90.8%. TaSe_3 was chemically exfoliated by sonicating 6 mg of powdered TaSe_3 crystals in 10 mL ethanol for 4 h, resulting in a brownish-black suspension. This suspension was then centrifuged at 2600 rpm for 15 min, leaving well-dispersed TaSe_3 wires 30 to 80 nm wide in the supernatant.

Acknowledgements

This project was supported, in part, by the by the Emerging Frontiers of Research Initiative (EFRI) 2-DARE project: Novel Switching Phenomena in Atomic MX_2 Heterostructures for Multifunctional Applications (NSF EFRI-1433395). The nano-device fabrication and characterization work at UC Riverside was also supported, in part, by the Semiconductor Research Corporation (SRC) and Defense Advanced Research Project Agency (DARPA) through STARnet Center for Function Accelerated nanoMaterial Engineering (FAME). The quasi-1D TaSe_3 devices were fabricated in the UCR Center for Nanoscale Science and Engineering (CNSE). The authors acknowledge useful discussions on $1/f$ noise with Dr. Michael Levinshtein (Ioffe Institute, St. Petersburg, Russia).

Author Contributions

A.A.B. conceived the idea, coordinated the project, and contributed to experimental data analysis; T.T.S. supervised material synthesis and contributed to materials analysis; G.L. fabricated and tested devices, analyzed experimental data, and conducted part of the low-frequency noise measurements; M.A.B. synthesized TaSe_3 and conducted materials characterization; S.L.R. conducted noise measurements and analyzed experimental data; M.S.S. and M. L. contributed to data analysis. All authors contributed to writing of the manuscript.

Supplementary Information:

Details concerning device fabrication are available on the journal web-site for free-of-charge.

TABLE I: E_A and E_p Extracted from $1/f$ Noise Measurements for Different Technologies

Technology	E_p (eV) - D-H model	E_A (eV) Empirical Model
Cu direct etch	1.10 [24]	
Cu with TaNTa barrier	0.76-0.78 [24]	0.79 [38]
Al	0.69 [21]	
Al – Si (1%)	0.80 [21]	
Al – Cu (4%)	0.89 [21]	
Al thin film		1.14 [22]
Al – Si (0.8%) passivated		0.74 [39]
Al – Si (1%) – Cu (0.5%) passivated		0.78 [39]
TaSe ₃	1.01 [this work]	0.88 [this work]

1. Novoselov, K. S.; Mishchenko, A.; Carvalho, A.; Castro Neto, A. H. 2D Materials and van der Waals Heterostructures. *Science*, **2016**, 353, 9439-1-11.
2. Geim, A.K.; Grigorieva, I.V., Van der Waals Heterostructures, *Nature*, **2013**, 499, 419-425.
3. Novoselov, K.S.; Geim, A.K.; Morozov, S.V.; Jiang, D.; Zhang, Y.; Dubonos, S.V.; Grigorieva, I.V.; Firsov, A.A., Electric Field Effect in Atomically Thin Carbon Films. *Science*, **2004**, 306, 666-669.
4. Zhang, Y.B.; Tan, Y.W.; Stormer, H.L.; Kim, P. Experimental Observation of The Quantum Hall Effect and Berry's Phase In Graphene. *Nature*, **2005**, 438, 201-204.
5. Balandin, A.A. Thermal properties of graphene and nanostructured carbon materials, *Nature Materials*, **2011**, 10, 569 - 581.
6. Li, L.; Yu, Y.; Ye, G. J.; Ge, Q.; Ou, X.; Wu, H.; Zhang, Y. Black Phosphorus Field-Effect Transistors. *Nat. Nanotechnol.* **2014**, 5, 372–377.
7. Teweldebrhan, D., Goyal, V., Balandin, A.A., Exfoliation and characterization of bismuth telluride atomic quintuples and quasi-two-dimensional crystals, *Nano Letters*, **2010**, 10, 1209.
8. Radisavljevic, B.; Radenovic, A.; Brivio, J.; Giacometti, V.; Kis, A. Single-layer MoS2 Transistors. *Nat. Nanotechnol.* 2011, 6, 147–150.
9. Cui, X.; Lee, G.H.; Kim, Y.D.; Arefe, G.; Huang, P.Y.; Lee, C.H.; Chenet, D.A.; Zhang, X.; Wang, L.; Ye, F.; Pizzocchero, F.; Jessen, B.S.; Watanabe, K.; Taniguchi, T.; Muller, D.A.; Low, T.; Kim, P.; Hone, J. Multi-Terminal Transport Measurements of MoS2 Using A van der Waals Heterostructure Device Platform. *Nature Nanotechnology*, **2015**, 10(6), 534-540.
10. Butler, S. Z.; Hollen, S. M.; Cao, L.; Cui, Y.; Gupta, J. A.; Gutiérrez, H. R.; Heinz, T. F.; Hong, S. S.; Huang, J.; Ismach, A. F. et al. Progress, Challenges, and Opportunities in Two-Dimensional Materials Beyond Graphene. *ACS Nano*, **2013**, 7, 2898– 2926.
11. Liu, G., Debnath, B., Pope, T.R., Lake, R.K., Salguero, T.T., Balandin, A.A., *Nature Nanotechnology*, **2016**, 11, 845.
12. Wang, Q. H.; Kalantar-Zadeh, K.; Kis, A.; Coleman, J. N.; Strano, M. S. Electronics and Optoelectronics of Two-Dimensional Transition Metal Dichalcogenides. *Nat. Nanotechnol.*, **2012**, 7, 699– 712.
13. Jariwala, D.; Sangwan, V. K.; Lauhon, L. J.; Marks, T. J.; Hersam, M. C. Emerging Device Applications for Semiconducting Two-Dimensional Transition Metal Dichalcogenides. *ACS Nano*, **2014**, 8, 1102– 1120.

14. Ferrari, A. C.; Bonaccorso, F.; Falko, V.; Novoselov, K. S.; Roche, S.; Boggilt, P.; Borini, S.; Koppens, F.; Palermo, V.; Pugno, N. Science and Technology Roadmap for Graphene, Related Two-Dimensional Materials and Hybrid Systems. *Nanoscale*, **2015**, 7, 4598–4810.
15. Lipatov, A.; Wilson, P.M.; Shekhirev, M.; Teeter, J.D.; Netusil, R.; Sinitskii, A., Few-layered titanium trisulfide (TiS₃) field-effect transistors. *Nanoscale*, **2015**, 7(29), 12291-12296.
16. Island, J.O.; Buscema, M.; Barawi, M.; Clamagirand, J.M.; Ares, J.R.; Sanchez, C.; Ferrer, I.J.; Steele, G.A.; van der Zant, H.S.J.; Castellanos-Gomez, A., Ultrahigh Photoresponse of Few-Layer TiS₃ Nanoribbon Transistors, *Adv. Opt. Mat.*, **2014**, 2, 641-645.
17. Island, J.O.; Barawi, M.; Biele, R.; Almazan, A.; Clamagirand, J.M.; Ares, J.R.; Sanchez, C.; van der Zant, H.S.J.; Alvarez, J.V.; D'Agosta, R.; Ferrer, I.J.; Castellanos-Gomez, A., TiS₃ Transistors with Tailored Morphology and Electrical Properties. *Adv. Mat.*, **2015**, 27(16), 2595-2601.
18. Stolyarov, M. A.; Liu, G.; Bloodgood, M. A.; Aytan, E.; Jiang, C.; Samnakay, R.; Salguero, T. T.; Nika, D. L.; Rumyantsev, S. L.; Shur, M. S.; Bozhilove, K. N.; Balandin, A. A. Breakdown Current Density in h-BN-Capped Quasi-1D TaSe₃ Metallic Nanowires: Prospects of Interconnect Applications. *Nanoscale*, **2016**, 8, 15774-15782.
19. Balandin, A.A., *Nature Nanotechnology*, **2013**, 8, 549-555.
20. von Haartman, M.; Ostling, M. Low-Frequency Noise in Advanced MOS Device; Springer: The Netherland, 2007.
21. Koch, R. H.; Lloyd, J. R.; Cronin, J. 1/f Noise and Grain-Boundary Diffusion in Aluminum and Aluminum Alloys. *Phys. Rev. Lett.*, **1985**, 55, 2487-2490.
22. Chen, T.-M.; Yassine, A. M. Electrical Noise and VLSI Interconnect Reliability. *IEEE Trans. on Electron Dev.*, **2002**, 41, 2165-2172.
23. Neri, B.; Diligenti, A.; Bagnoli, P. E. Electromigration and Low-Frequency Resistance Fluctuations in Aluminum Thin-Film Interconnections. *IEEE Trans. on Electron Dev.*, **1987**, 34, 2317-2322.
24. Beyne, S.; Croes, K.; De Wolf, I.; Tókei, Zs. 1/f Noise Measurements for Faster Evaluation of Electromigration in Advanced Microelectronics Interconnections, *J. Appl. Phys.*, **2016**, 119, 184302-1-8.
25. Vandamme, L. K. J. Noise as a Diagnostic Tool for Quality and Reliability of Electronic Devices. *IEEE Trans. on Electron Dev.*, **1994**, 41 2176-2187.

26. Neri, B.; Ciofi, C.; Dattilo, V. Noise and Fluctuations in Submicrometric Al-Si Interconnect lines, *IEEE Trans. on Electron Dev.*, **1997**, 44, 1454-1459.
27. Guo, J.; Jones, B. K; Trefan, G. The Excess Noise in Integrated Circuit Interconnects Before and after Electromigration Damage. *Microelectron Reliab.*, **1999**, 39, 16771690.
28. Liu, G.; Rumyantsev, S.; Shur, M. S.; Balandin, A. A. Origin of 1/f Noise in Graphene Multilayers: Surface vs. Volume. *Appl. Phys. Lett.*, **2013**, 102, 093111-1-5; Rumyantsev, S.; Liu, G.; Stillman, W.; Shur, M.; Balandin, A. A. Electrical and Noise Characteristics of Graphene Field-Effect Transistors: Ambient Effects, Noise Sources and Physical Mechanisms. , *J. Phys.: Condens. Matter.*, 2010, 22, 395302-395307.
29. Rumyantsev, S.L., Jiang, C., Samnakay, R., Shur, M.S., Balandin, A.A., 1/f Noise characteristics of MoS₂ thin-film transistors: Comparison of single and multilayer structures, *Electron Device Letters*, **2015**, 36, 517.
30. Snow, E. S.; Novak, J. P.; Lay, M. D.; Perkins, F. K. 1/f Noise in Single-Walled Carbon Nanotube Devices. *Appl. Phys. Lett.*, **2004**, 85, 4172-4174.
31. Rumyantsev, S.; Vijayaraghavan, A.; Kar, S.; Khanna, A.; Soldano, C.; Pala, N.; Vajtai, R.; Nalamasu, O.; Shur, M.; Ajayan, P. 14 International Symp. "Nanostructures: physics and technology", St. Petersburg, June 26-30, 2006.
32. Vijayaraghavan, A; Kar, S.; Rumyantsev, S.; Khanna, A.; Soldano, C.; Pala, N.; Vajtai, R.; Kanzaki, K.; Kobayashi, Y.; Nalamasu, O.; Shur, M.; Ajayan, P. *J. Appl. Phys.*, **2006**, 100, 024315
33. Shur, M.; Rumyantsev, S.; Liu, G.; Balandin, A. A. Electrical and Noise Characteristics of Graphene Field-Effect, (invited), ICNF 2011, Toronto, Canada, June 12-16 2011, Proc.: IEEE Xplore 145-149.
34. Xu, Y.; Huang, L.; Chen, G.; Wu, F.; Xia, W.; Liu, H. Electromigration — Induced Failure Mechanism and Lifetime Prediction in NiCu Thin Film. *Electronic Packaging Technology (ICEPT) 2014 15th International Conference on*, 2014, 1071-1074.
35. Dutta, P.; Horn, P. Low-Frequency Fluctuation in Solids: 1/f Noise. *Rev. Mod. Phys.*, **1981**, 53, 497-516.
36. Dutta, P., P. Dimon, and P. M. Horn, Energy Scales for Noise Processes in Metals. *Phys. Rev. Lett.*, **1979**, 43, 646-649.
37. Cottle, J. G.; Chen, T. M.; Rodbell, K. P. A Comparison between Noise Measurements and Conventional Electromigration Reliability Testing, Proc 26th Re1 Phys. Symp. 1988, 203-208.

38. Tang, B. J.; Croes, K.; Simoen, E.; Beyne, S.; Adelman, C.; Tókei, Zs. Experimental Validation of Electromigration by Low Frequency Noise Measurement for Advanced Copper Interconnects Application. *Noise and Fluctuations (ICNF), 2015 International Conference on*, 2015, 1-4.
39. Bagnoli, P. E.; Ciofi, C.; Neri, B.; Pennelli, G. Electromigration in Al Based Stripes: Low Frequency Noise Measurements and MTF Tests. *Microelectron. Reliab.*, **1996**, 36, 1045-1050.

Figure Captions

Figure 1: (a) High resolution scanning transmission electron microscopy image of exfoliated TaSe₃ showing pristine metal trichalcogenide chains that extend along the *b* axis. (b) Scanning electron microscopy image of TaSe₃ crystals prepared by CVT method. (c) SEM image of representative quasi-1D TaSe₃ devices.

Figure 2: Current-voltage characteristics of TaSe₃ devices with different channel length. The linear characteristics at low voltage indicates good Ohmic contact of TaSe₃ channel with the metal electrodes. The optical microscopy image of the devices is shown in the inset. The quasi-1D TaSe₃ channel (light blue) is covered with *h*-BN capping layer (green area), which acts as protection layer against oxidation and environmental exposure. The metal electrodes, in contact with TaSe₃ channel at the edges, are fabricated by etching through *h*-BN capping layer.

Figure 3: (a) Typical noise spectrum of TaSe₃ devices at room temperature. The noise spectrum S_I is flowing $1/f^\gamma$ dependence with $\gamma=1.1\sim 1.2$. The inset shows the noise level at $f=10$ Hz as the function of the channel (source-drain) current spanning from $0.2\ \mu\text{A}$ to $10\ \mu\text{A}$. The quadratic dependence of the noise spectrum density S_I on the channel current I indicates that the $1/f$ noise measured at this current level originates from the TaSe₃ device itself rather than the current induced effects. (b) Normalized noise spectrum density as a function of the resistance for different low-dimensional material systems - quasi-1D TaSe₃ nanowires, graphene and carbon nanotubes. For comparison, the empirical relation $A=10^{-11} R$ for the low-frequency noise versus resistance R derived from the carbon nanotube studies [29, 31-33] is also shown. The noise in quasi-1D TaSe₃ nanowires is about one order of magnitude lower than that in graphene.

Figure 4: Normalized noise spectra density S_I/I^2 measured for the quasi-1D TaSe₃ nanowire at different temperatures. The $1/f$ noise at room temperature becomes more of $1/f^2$ - type at elevated temperatures. The increased frequency power factor γ suggests the onset of the electromigration processes. The inset shows the temperature dependent resistance of the quasi-

1D TaSe₃ nanowire measured in the range from 300 K to 450 K. The gradual increase of the resistance with temperature, for $T < 410$ K is typical for metal. The sharply rising resistance for $T > 410$ K indicates the occurrence of electromigration.

Figure 5: (a) Extracted frequency power factor γ as the function of temperature. The frequency power factor γ increases from 1.16-1.24 at 298 K to 1.72-1.75 at 350 K, and remains approximately constant at 1.71-1.75 above 350 K. The blue curve is the fitting of the experimental data. (b) The evolution of the normalized noise spectra density S_I/I^2 with temperature T . The blue curve is calculated from the Dutta – Horn model. The activation energy estimated from the Dutta - Horn model is $E_P = 1.01$ eV.

Figure 6: Temperature dependent $1/f^2$ noise analysis using the Arrhenius plot of $T \times S_I/I^2$ versus $1000/T$. The extracted electromigration activation energy for quasi-1D TaSe₃ nanowire is $E_A = 0.88$ eV.

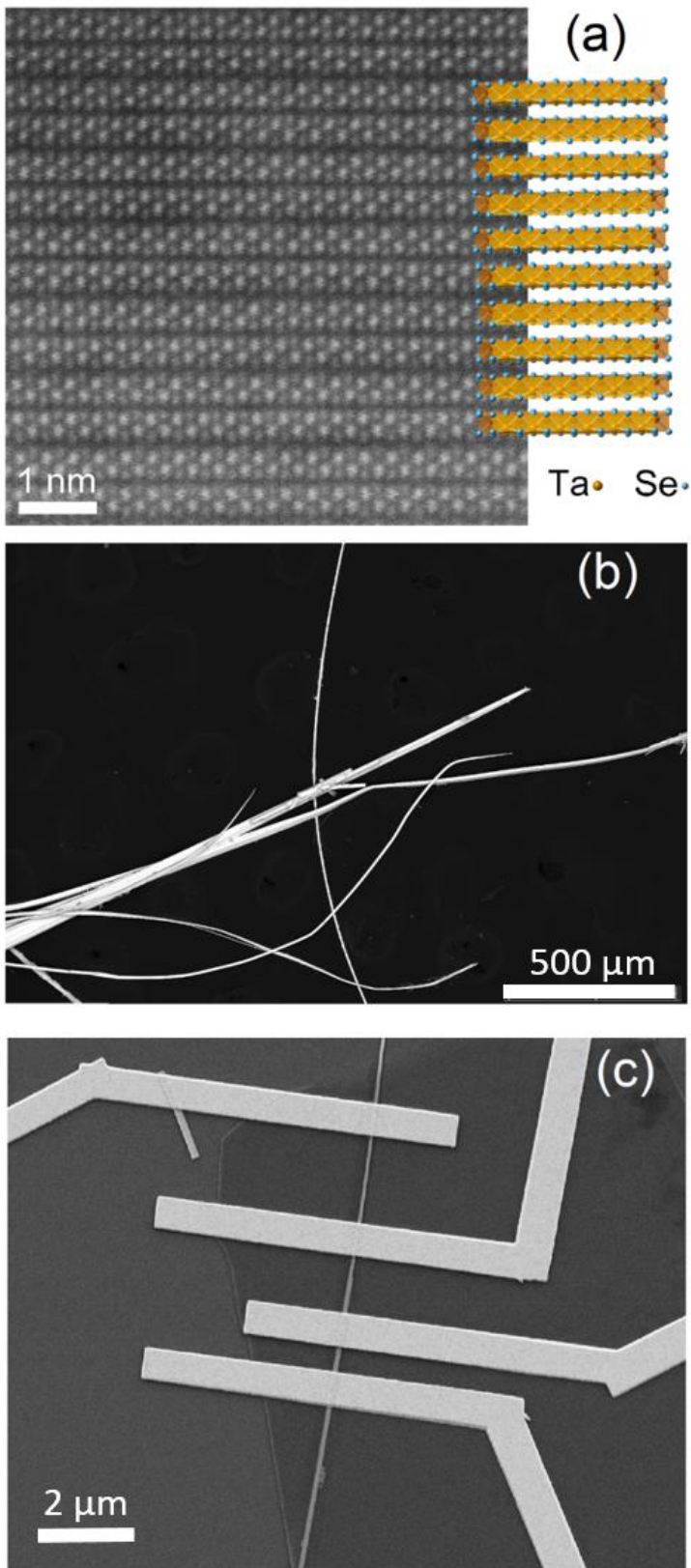


Figure 1

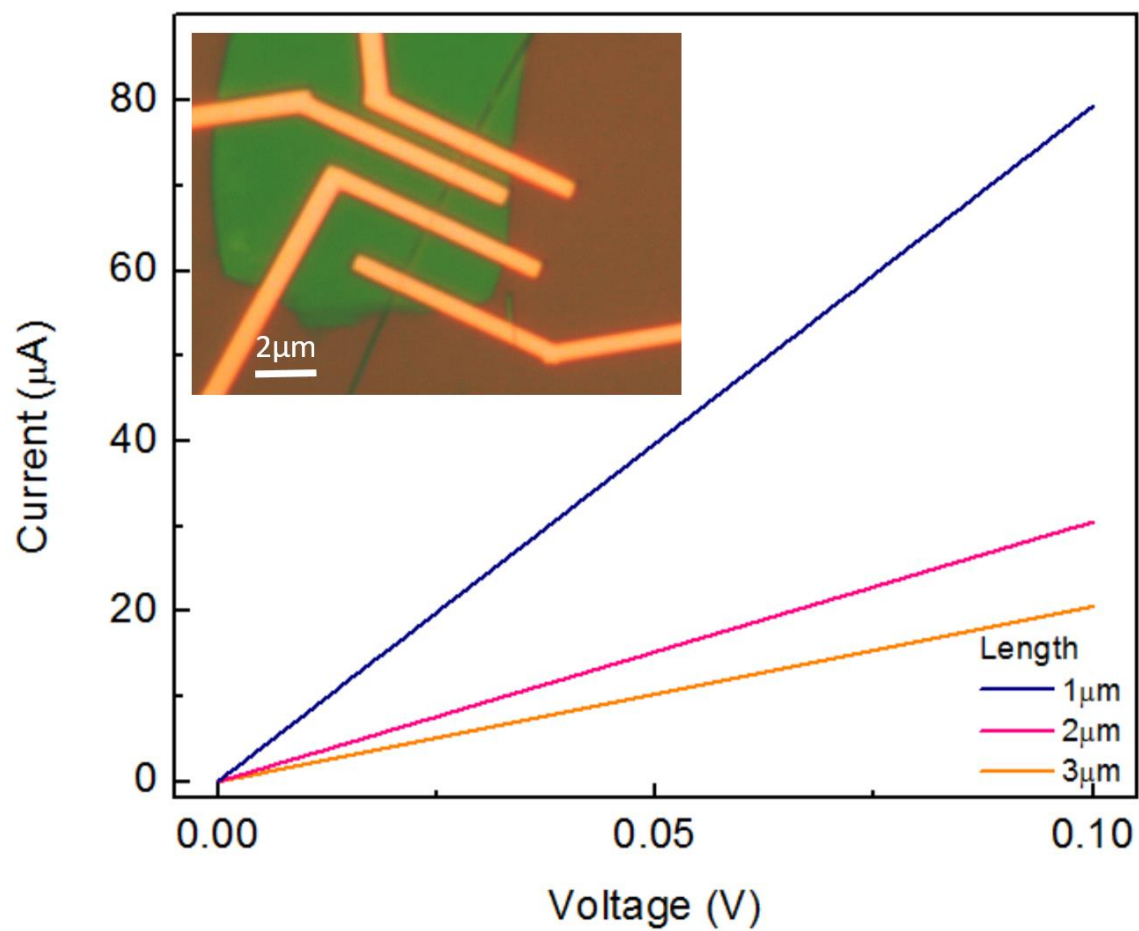


Figure 2

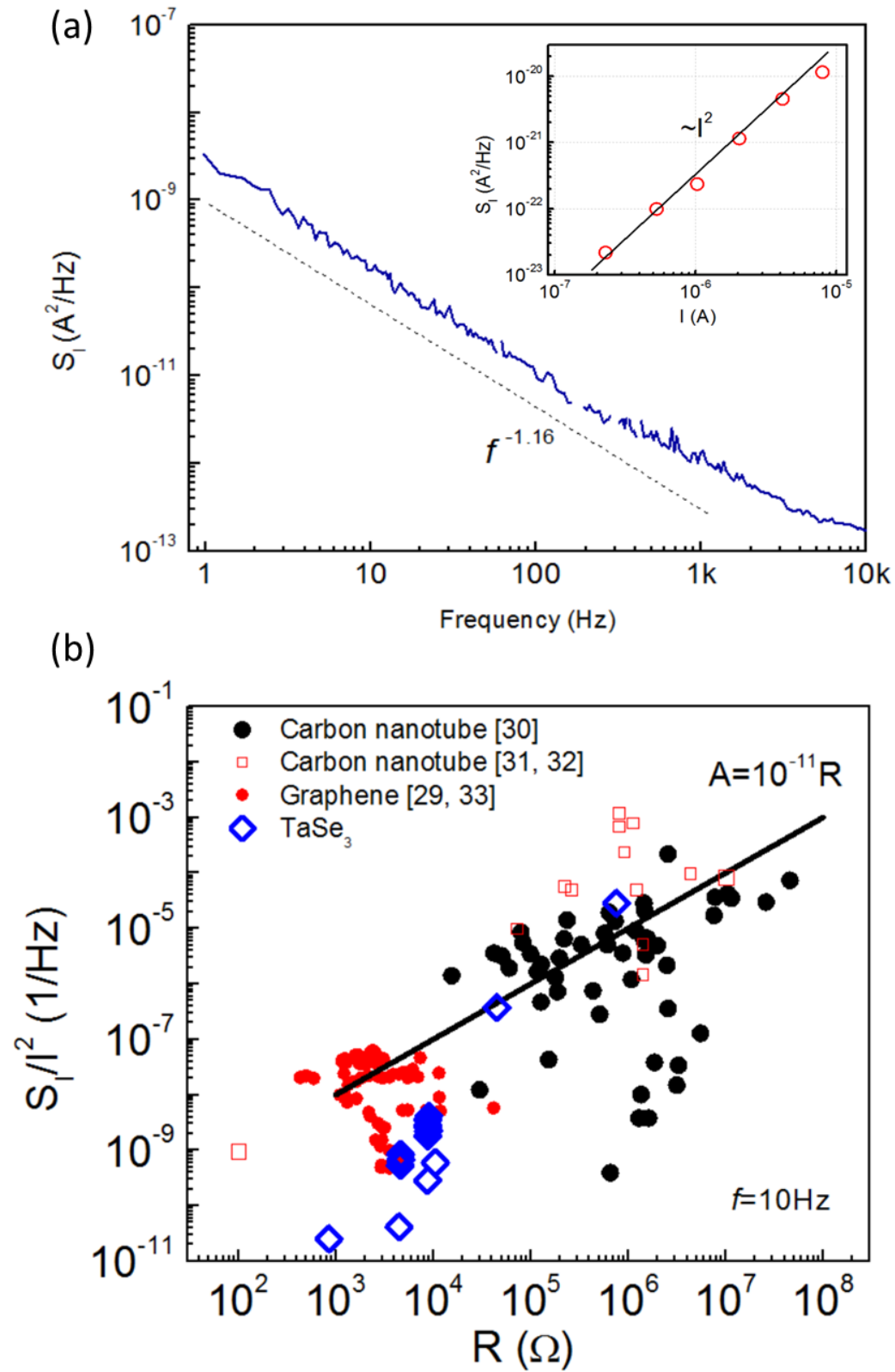


Figure 3

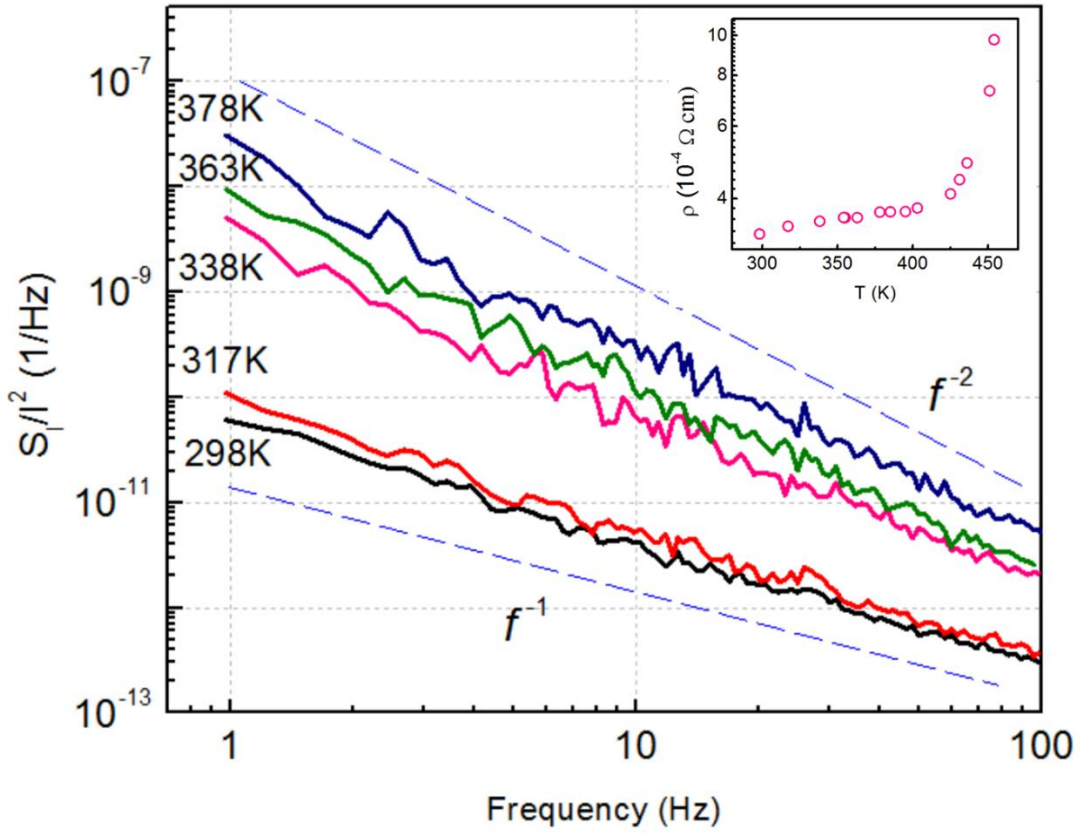


Figure 4

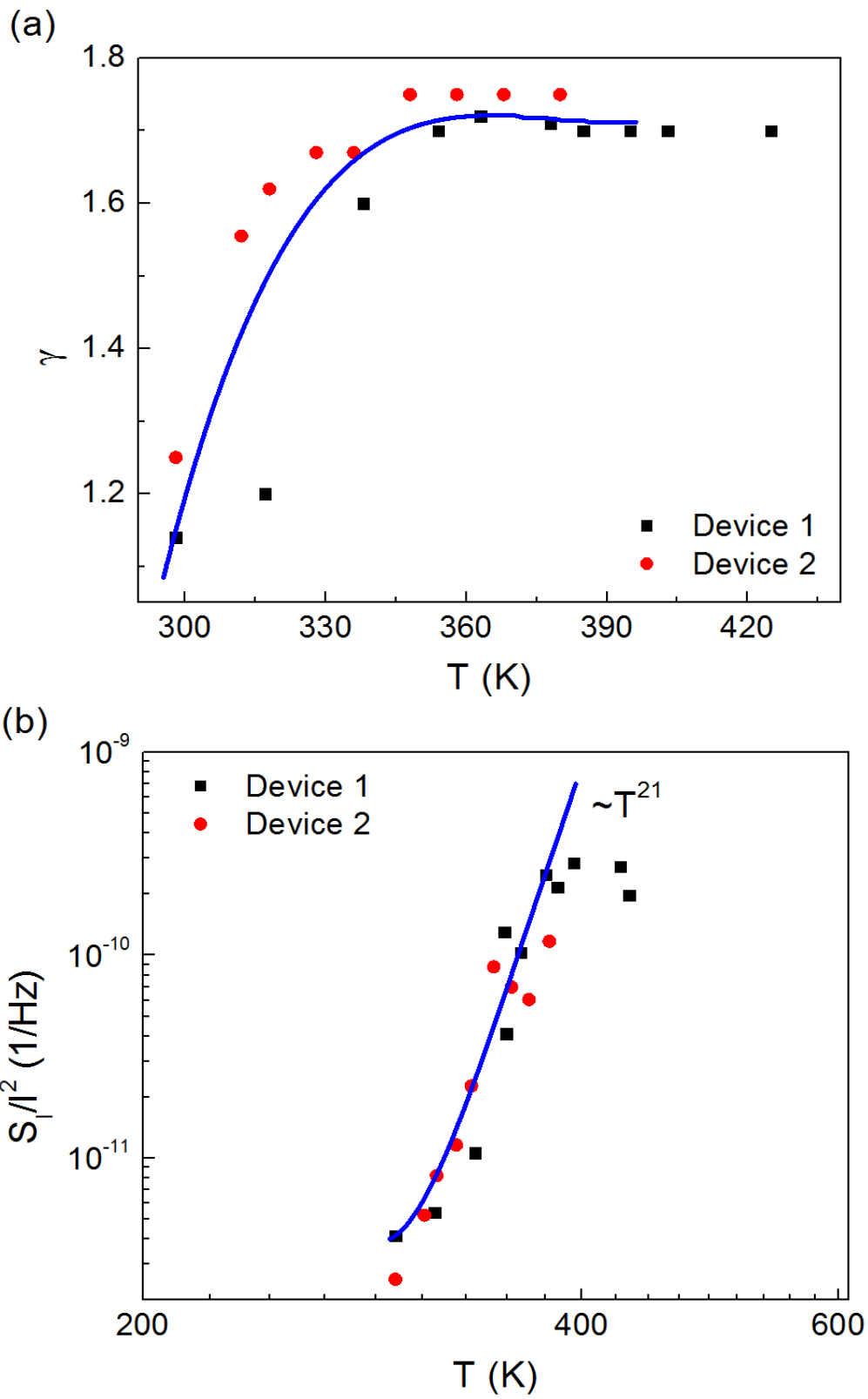


Figure 5

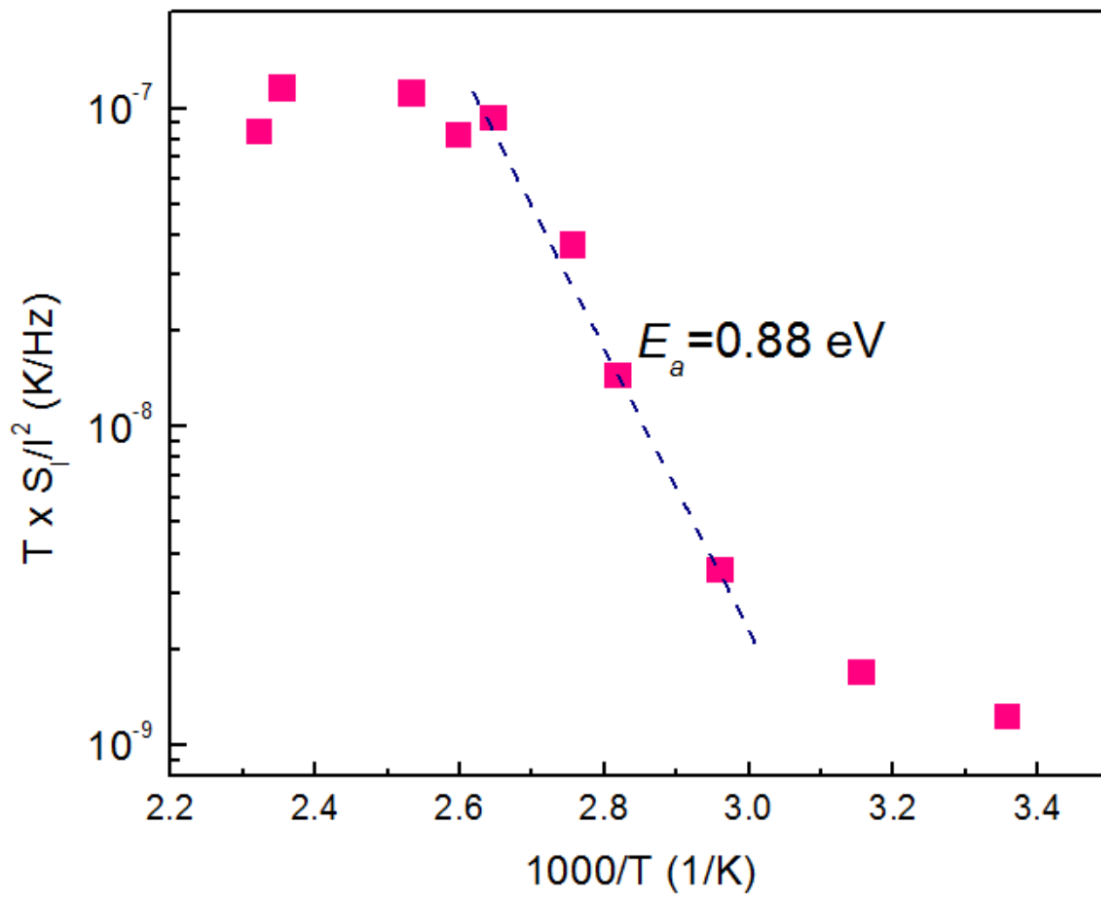


Figure 6